Stainless Steels Can Be Cathodically Protected Using Energy Stored at the Marine Sediment/ Seawater Interface

LEDA H. ORFEI, SILVIA SIMISON, AND
JUAN PABLO BUSALMEN*

*Laboratorio de Bioelectroquímica, División Corrosión,
INTEMA−CONICET, Universidad Nacional de Mar del Plata,
Juan B. Justo 4302, B7608FDQ Mar del Plata, Argentina*

Laboratory-scale experiments were performed in which the corrosion protection of stainless steels in seawater was afforded by cathodic protection. The method was implemented for the first time using the potential difference at the marine sediment/seawater interface as the only source of electric power. Graphite electrodes buried in marine sediment, developing a potential of −0.45 V versus a saturated calomel electrode (SCE), were used as anodes to cathodically polarize UNS S30403 stainless steel coupons that were exposed to seawater. The cathodic protection system was operated with low polarization of stainless steel, typically to −0.2 V (vs SCE) and was found to properly prevent material failure even in the presence of a well-developed biofilm. With voltammetry, the protection current was found to be related to the oxidation of reduced sulfur compounds in the sediments. Results demonstrate that this inexpensive and environmentally friendly method can, so far, extend the service life of stainless steels in seawater.

Introduction

Stainless steels (SS) are recognized by their very high resistance to corrosion. This feature is the result of the presence of a protective surface film composed mainly of iron and chromium oxides that acts as a passivating barrier to charge transfer (and corrosion). The potential range of film presence and stability is recognized as the passive region and extends from the potential of oxides formation to the pitting or breakdown potential at which the rupture of the oxide film determines the localized corrosion failure.

When SS are immersed in seawater, a biofilm is readily formed on their surface inducing a shift of the open circuit potential to positive (anodic) values (*1−4*). This phenomenon, called potential ennoblement, is thought to be caused by the increase in the cathodic half-cell reaction of corrosion processes as a consequence of microbial activity. Although a general explanation has not been fully defined yet, all the proposed mechanisms for the potential ennoblement include the participation of a cathodic depolarizer. Increased cathodic currents are attributed to the reduction of biogenic MnO_2 (*5*), hydrogen peroxide (*4, 6*), or microbial catalysis of oxygen reduction (*3, 7*). At potentials beyond the pitting potential,

the electrons demanded by the increased reduction reactions are provided by an increased rate of metal dissolution at the oxide film failure sites as the anodic counterpart of the so-called microbiologically influenced corrosion (MIC) process. Regardless of the increased cathodic currents resulting from the presence of MnO_2 or peroxide or from the oxygen reduction catalysis, the ennoblement process can be counteracted by electrochemical polarization preventing material failure.

Within most widely used corrosion prevention methods is cathodic protection (CP). This method is based on the cathodic (negative) polarization of the structure to be protected by coupling to a more active (anodic) metal (galvanic or sacrificial anodes protection method) or to a dc power source (impressed current method). Electrons needed for the reduction reaction on the cathode are provided by the dissolution of the sacrificial anode in the former method or by the power source in the later one. With a proper design, the oxidation rate on the structure can be restricted to a negligible level (*8*).

Reimers et al. (2001) (*9*) had demonstrated that electrical energy can be obtained by installing electrodes at both sides of the marine sediment/seawater interface in a fuel cell-like arrangement. They proposed that this energy could be used to power low amperage devises for long time. On the basis of this data, the objectives of this work were to evaluate if this new power source can be used to cathodically protect SS from corrosion and to investigate the reactions involved in current generation.

We report here the results of long-term experiments in which SS coupons immersed in seawater were electrically connected to buried graphite electrodes through an external circuit. Results clearly show that this connection allowed enough cathodic polarization to prevent the ennoblement effects of microbial colonization and to prevent corrosion failure. Protection is afforded even in the presence of a completely developed biofilm on SS coupons. Cyclic voltammetry, scanning electron microscopy (SEM), and energy dispersive X-ray microanalysis (EDX) were used to investigate the origin of protection current. We demonstrate that the oxidation of reduced sulfur compounds in the sediment is one of the energy-providing processes and propose the use of sediment anodes as a novel cathodic protection method.

Experimental Section

Experimental Device and Electrodes. Experiments were done in a laboratory scale water/sediment flow system using sediment and seawater collected from a fuel oil discharge site at the Mar del Plata port (a detailed description of the experimental setup is provided in the Supporting Information). Two kinds of experiments were performed, three replicates in which the entire system was operated during 15−20 days to allow the sediment stabilization before connecting the electrodes, and a fourth experiment aimed to analyze a nonstabilized sediment in which the electrodes were connected after 24 h of sediment collection.

Graphite electrodes were constructed from bars of 0.7 cm in diameter and 5 cm in length. The electric contact was made on one side using silver epoxy resin, and the whole contact was mounted in a PVC holder and covered with acrylic resin. The total exposed graphite area was 11 cm^2. Before use, the electrodes were cleaned by immersion in 0.3 N HCl and rinsed gently with distilled water.

UNS S30403 stainless steel coupons of 5 × 7 cm were cut from 0.3 cm thick sheets and abraded with emery paper to grade 400. The electric contact was made on one side using

* Corresponding author present address: Universidad de Alicante. Dpto. de Química Física. Fac. de Ciencias 1. Ca. de Alicante s/n. 03690, San Vicente del Raspeig, España; e-mail: jbusalme@fi.mdp.edu.ar; phone: +34 965903536; fax: +34 965903537.

a stainless steel wire secured through a hole. Samples were suspended leaving the contact site out of the water to minimize crevice initiation at this site. The SS exposed area was 50 cm².

Graphite electrodes were buried 15 cm below the sediment/seawater interface and connected as protecting anodes to SS coupons (cathodes) that were partially immersed in the water. Electrical coupling was done through adjustable resistors of 5−100 kΩ. After connection, the potential of the SS cathodes was set at −0.2 V by changing the resistor value. The reference electrode was a saturated calomel electrode (SCE), and all potentials are reported against this reference. For the experiments with nonstabilized sediment, the protection was implemented using a fixed resistor of 5 kΩ. During every experiment, a total of 16 SS coupons and an equal number of graphite electrodes were installed. Half were connected to implement the cathodic protection arrangements, and the other half were used as nonconnected controls.

Electrochemical Measurements. The potential of anodes and cathodes was continuously monitored using a 16 channel data collection interface connected to a personal computer and controlled by a homemade acquisition software. The galvanic current circulating by the external circuit was calculated from the potential difference between anodes and cathodes using Ohm's law. For experiments with the nonstabilized sediment, the potentials were measured daily using an HP 34401A multimeter. Direct measurements of galvanic current were also periodically performed with the same equipment.

Cyclic voltammetry was performed in situ every week on active (anodes) and control graphite electrodes. The potential was scanned between the open circuit potential (OCP) reached by the electrode after disconnection from the cathodic protection system and 0.35 V as the upper potential limit, starting anodically from the OCP. The scan rate was of 0.01 V s⁻¹.

At the end of the cathodic protection experiments, a voltammetric analysis within the whole scanning potential range (−1.3 to 0.45 V) was performed on active and control graphite electrodes as described before. The scan rate was 0.002 V s⁻¹ in this case to improve the analysis resolution.

A large-area platinum mesh immersed in the seawater was used as the counter electrode during all the experiments.

Microscopy. Microbial colonization of SS coupons was verified by optical microscopy. Samples were periodically extracted, washed carefully by immersion in seawater to eliminate loosely adhered material, air-dried, and observed at 50× and 200× magnification in an Olympus PMG3 metallurgical microscope equipped with a CCD (charge-coupled device) camera. At the end of the experiments, SS samples were scraped and washed gently with distilled water to remove the biological material, degreased with alcohol, air-dried, and observed at 200× magnification to determine the presence of localized corrosion.

Scanning Electron Microscopy (SEM) and Energy Dispersive X-ray Microanalysis (EDX). At the end of the experiments the surface of active and control graphite electrodes was analyzed by SEM and EDX using a Phillips 515 scanning electronic microscope equipped with a Falcon PV8200 EDX detector. Samples were extracted from the sediment, washed with distilled water to remove the loosely adhered sediment, air-dried, and sputtered under vacuum for deposition of Ag vapors.

Results

Cathodic Protection Experiments. The results in Figure 1 show the typical evolution of potential for SS coupons (cathodes) and buried graphite electrodes (anodes) connected through a variable resistor, together with the potential
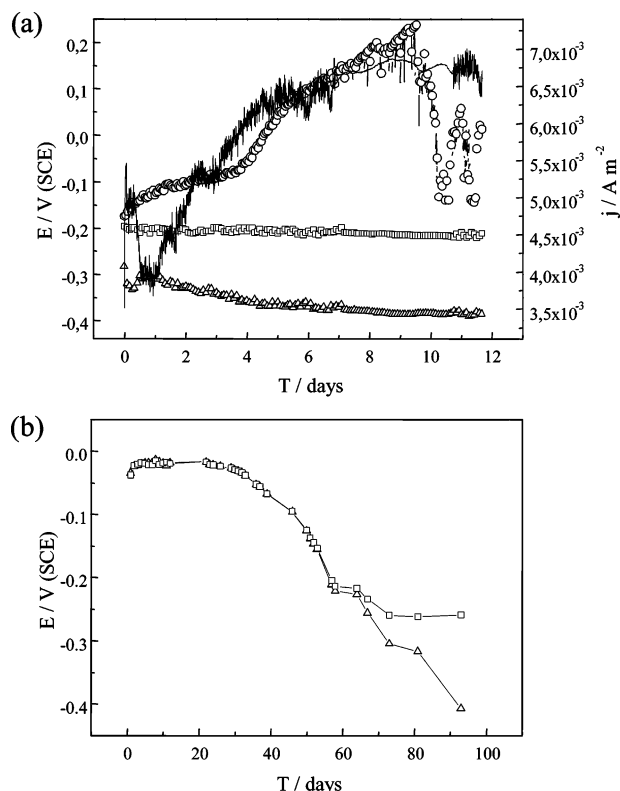
FIGURE 1. Evolution of electrodes potential in a cathodic protection arrangement composed of (□) stainless steel cathodes immersed in seawater and (△) graphite anodes buried in the underlying sediment with (a) 20 days and (b) 24 h of sediment stabilization before electrode connection. ○ represents the open circuit potential of a stainless steel coupon. The solid line represents the galvanic current density by unit cathode area calculated from the potential difference between anode and cathode using Ohm's law. The cathodic protection was operated at a fixed potential of −0.2 V in panel a. In panel b, a fixed resistance of 5 kΩ was used.

changes for nonconnected SS used as control. Connection of electrodes was done after 20 days (panel a) or after 24 h (panel b) of sediment stabilization.

The corrosion potential of nonconnected SS showed a typical ennoblement curve reaching values of up to 0.22 V after 8−9 days of exposure (Figure 1a). Following ennoblement, potential suddenly drops down to negative values because of the initiation of localized corrosion (6, 10). The potential of SS electrodes connected to graphite anodes remained without change at the initially adjusted potential of −0.2 V until the end of the experiment (120 days) (Figure 1a).

Unconnected graphite electrodes buried in stabilized sediment rapidly adopted an open circuit potential of around −0.45 V that remained with little changes during the experiment (data not shown). Graphite electrodes in the same sediment but connected to SS coupons, were depolarized to near −0.3 V immediately after connection and progressively returned to more negative values reaching a final potential of around −0.4 V (Figure 1a).

When electrodes were installed in nonstabilized sediment, the potential of both the cathodes and anodes suddenly changed to a common value at −0.07 ± 0.02 V after connection (Figure 2b). The potential difference between them remained with low variation during the first 40−50 days of the experiment. After which, it progressively increased while the potential of both the cathodes and anodes changed gradually to lower values. Cathodes reached a plateau at a potential of around −0.25 ± 0.05 V, while the potentials of anodes were around −0.4 V after 90 days of experiment
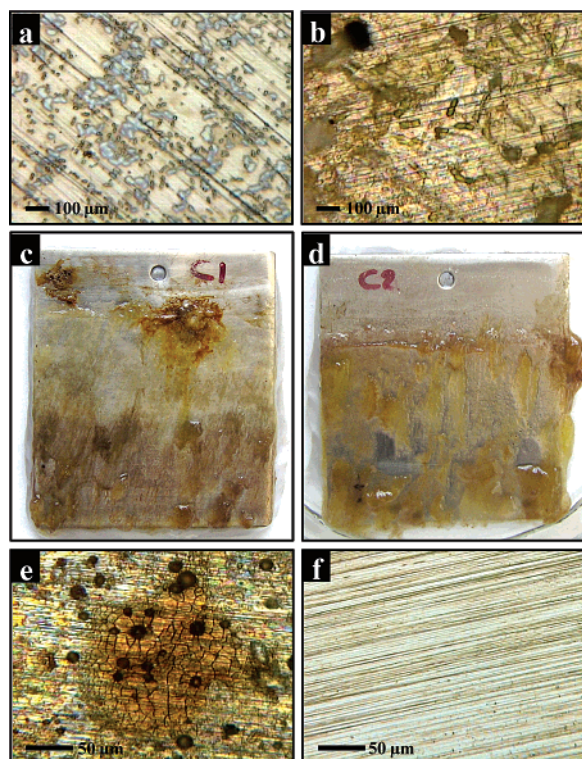
FIGURE 2. Microbial colonization observed on stainless steel coupons after (a) 24 h, (b) 10 days, and (c) 120 days of exposure to seawater at the open circuit potential and (d) after 120 days polarized at −0.2 V by connection with a buried graphite electrode. Panels e and f are micrographs of the surfaces in c and d after biofilm removal, showing the pitting corrosion attack and the absence of corrosion, respectively. The magnification for panels a and b is 50×, and that for panels e and f is 200×.

FIGURE 3. Cyclic voltammetries performed on graphite electrodes buried in marine sediment during (—) 21, (· · ·) 56 and (- - -) 84 days (a) at the open circuit potential and (b) connected as an anode to protect a stainless steel coupon.

(Figure 1b). Ennoblement of nonconnected SS was evident in this case after 10 days of exposition and reached maximal values after 40 days of experiment (data not shown). Control anodes rapidly adopted a potential of −0.35 V that gradually decreased to final values of around −0.40 V (data not shown).

The adhesion of microorganisms and the growth of biofilms were evident on both the connected and control SS samples during all the experiments. Within the first 24 h of exposure, the coupons were rapidly colonized by microorganisms (Figure 2a). After 6−20 days, a more abundant colonization was observed that included photosynthetic microscopic algae (Figure 2b). Beyond 30 days of exposure, a complex biofilm with macroscopic dimensions was observed, and it grew to completely cover the immersed SS area by the end of the experiments (Figure 2c and d).

Typical values of galvanic current flowing between graphite anodes and SS cathodes when the experiments were done with the stabilized sediment are shown in Figure 1a. Current densities (referred to cathode area) where initially of 4×10^{-3} A m^{-2}. During the first 10 days, they increased to values of up to 7×10^{-3} A m^{-2} and remained around this value with low variations for the rest of the experiment.

At the end of the exposure, the SS coupons were inspected for localized corrosion. Corrosion failure of unprotected samples was evident from the accumulation of corrosion product in the biofilm (Figure 2c) and also from the numerous pits observed during a microscopic inspection after the biofilm was removed (Figure 2e). The samples that were connected to graphite anodes, on the other hand, showed no evidence of corrosion at either the direct observation (Figure 2d) or the microscopic level (Figure 2f).

Energy-Providing Processes. To investigate the anodic processes involved in current generation, voltammetric
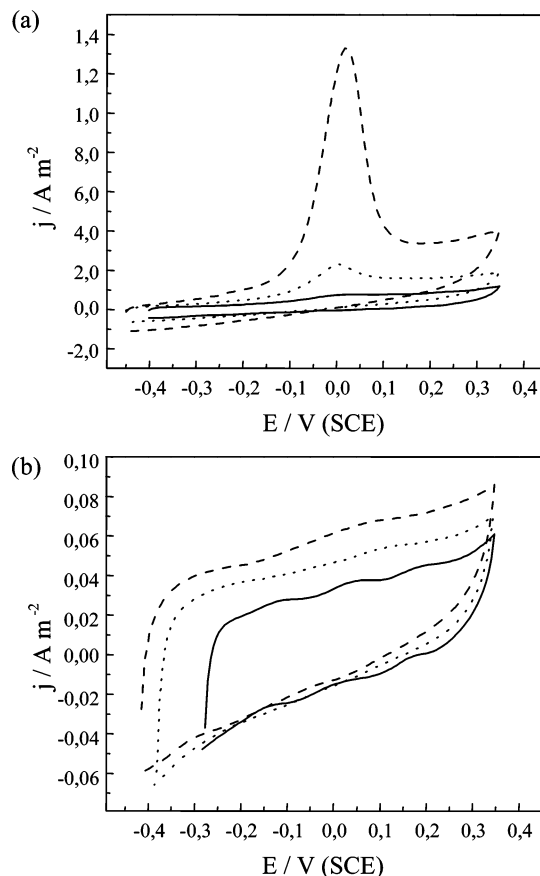
curves were periodically recorded on both control and active graphite electrodes during experiments with the nonstabilized sediments. As shown in Figure 3a, there is an oxidation process with a peak potential of around 0.00 V. Peak current densities increase with time reaching values higher than 1.3 A m^{-2} after 84 days. This peak was not detected on graphite electrodes that were connected as anodes to protect SS (Figure 3b). Oxidation processes in this case were characterized by an increase in the anodic current measured throughout the forward scan of the whole potential range explored (Figure 3b). It is important to note that scans started at progressively lower potential values because of a cathodic shift in the steady-state potential reached by the anodes after disconnection. Currents were, in this case, much lower than those recorded on control electrodes.

To further analyze redox processes on graphite electrodes buried in the sediment, new voltammetric assays were performed at the end of the cathodic protection experiments, in which the potential was scanned between −1.3 and 0.45 V. Current profiles recorded during the first two potential cycles of the experiments are shown in Figure 4. For control (nonconnected) electrodes, the oxidation peak reported in Figure 3 was again recorded during the first forward scan. In the backward excursion, two reduction waves with peak potentials of around −0.8 V and −1.0 V were observed (Figure 4a). During the second forward scan, new oxidation peaks were detected at potentials of around −0.8 and −0.3 V, in addition to that found during the first cycle that was shifted approximately 50 mV to higher potential values, as compared to that in Figure 3a. On graphite anodes used for cathodic protection, a first forward scan without oxidation peaks (inset Figure 4b) was followed by a backward scan showing only
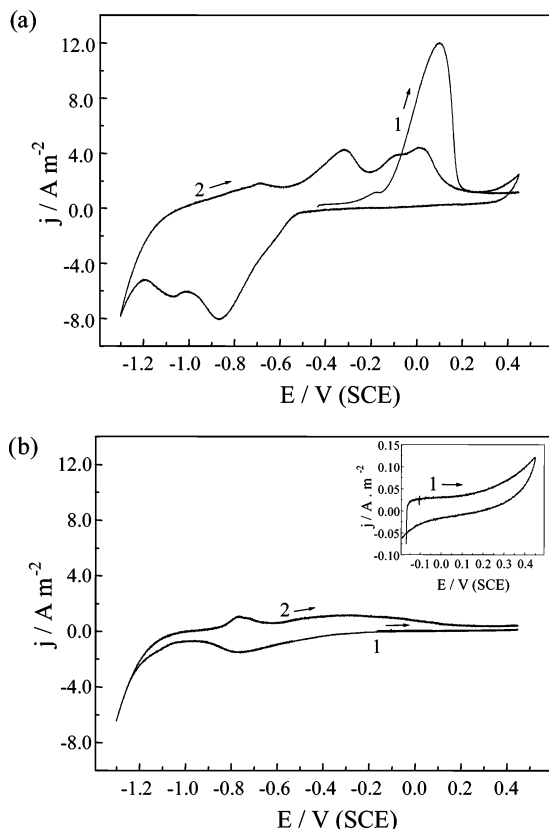
FIGURE 4. Cyclic voltammetries performed on graphite electrodes buried in marine sediment during 120 days (a) at the open circuit potential and (b) connected as an anode to protect a stainless steel coupon. The arrows indicate the first (1) and second (2) voltammetric cycle.

one reduction wave at around -0.75 V (Figure 4b). An oxidation peak at -0.75 V and a broad oxidation wave from -0.6 to 0.0 V were observed during the second forward scan (Figure 4b).

Additional information obtained by SEM and EDX analyses about the surface of control and active anodes is given in the Supporting Information.

Discussion

When polarized to the half-cell potential of the metal ion redox processes, a metallic material has a corrosion rate of zero because the rate of the deposition reaction is the same as the dissolution one and the net reaction is zero. Nevertheless, although desirable, the polarization needed to reach the half-cell potential of most of the alloys used in industrial applications may sometimes be energy consuming in excess. Fortunately, the corrosion rate of these materials may often become acceptable with a lesser cathodic polarization (*11*).

Different criteria have been applied to determine the degree of polarization needed to reduce corrosion to an acceptable rate (*8, 11*), but the most common value and the one most widely used in practice is -0.805 V versus the silver/ silver chloride reference electrode (i.e., -0.827 (SCE)) (*8*). The selection of this value is based on the calculation of the half-cell potential for the dissolution of iron in neutral environments using the Nernst equation, and even when it is strictly applicable only for this material in these environments (*11*), it has been often taken as a reference for the protection of stainless steels in seawater (*12–18*). Main problems that arose in these cases were related to the extremely high current density needed to maintain polarization (*12, 13*) that was reported in some cases to be higher than that required to protect mild steel in seawater at the same potential (*18*). Hydrogen embrittlement has also been reported as a problem on cathodically protected 13% chromium stainless steels (*19, 20*).

Cathodic currents have been found to dramatically increase as a result of the development of a biological film on protected SS surfaces (*1, 18*). Moreover, the biologically catalyzed current increase has been observed to follow a relationship with the degree of polarization (*17, 18*). In addition, Babic and Meticoshukobic (1993) (*21*) showed that oxygen reduction is favored on SS at potentials below -0.5 V (SCE) because of the good catalytic properties of Cr_2O_3, which together with the biological effect clearly indicates that polarization to values under -0.5 V should be avoided when applying cathodic protection to SS. The question arises if these materials can be properly protected by polarizing them to more positive potentials.

As reported previously by Jonhsen and Bardall (1985) (*18*), for the case of high-alloy steels (254 SMO and Sanicro 28), cathodic protection can be applied at potentials as high as 0.1 V (SCE) with no risk of crevice corrosion initiation. This helps to lower the current requirements. In the experiments presented here on UNS S30403, protection was effectively implemented at -0.2 V (SCE) through the connection of SS to buried graphite anodes, thus avoiding the application of excessive polarization. The maximal requirement of current was markedly lower than that reported by others (*13, 15–17, 22*) (Figure 1), confirming that the prevention of corrosion can be afforded with a much lower energy investment and, most importantly, that this requirement can be fulfilled using energy obtained from a renewable reservoir. In accordance to previous results (*1, 18, 22, 23*), the protection current increased with the time of exposure (Figure 1) because of the action of microorganisms included in the biofilm that developed at the SS surface (Figure 2). The current increase was closely related to changes in the OCP of nonprotected SS, showing a common cause for these independent observations (Figure 1a). Additional evidence for the microbial catalysis of reduction processes on SS are provided in the Supporting Information. It is important to note that, even under this biologically increased current demand, anodic processes at the buried graphite electrode surface were able to effectively sustain the polarization of SS providing current densities of up to 7×10^{-3} A m^{-2} of cathode (Figure 1a).

The ennoblement degree is known to be dependent on environmental variables (*3, 23*), suggesting that a similar situation will be found for current demand when implementing a cathodic protection system in a real application. The balance between particular current requirements and the energy yield of buried anodes could be afforded by both adjusting the external load value and changing the area ratio upon which the cathodic and anodic reactions take place. It is important to note that, in the particular case of cathodic protection, the value of the external load applied to the system is dictated by the selected protection potential (i.e., -0.2 V) and not by the criteria of maximal power output as in fuel cell operation. This allows the adjustment of the area ratio to balance the system. During field experiments performed by others (*24*), a sustained power output of around 90×10^{-3} A m^{-2} was obtained from an active anode during more than a year. Although it is still unknown if this valuable data would be representative of the general case for marine sediments, current densities reported in Figure 1a suggest that the area of the structure to protect could be increased up to 12 times the anode area without risk of protection failure. Interestingly, a very recent report by Lowy et al. (*24*) showed that the use of modified anodes allowed charge-transfer kinetic limitations to be overcome at the anodic interface, rendering a five times higher current density yield than that obtained with plain graphite anodes. The development of this or other similar strategies for field applications would allow the

operational area ratio to be greatly increased for the cathodic protection strategy proposed here.

Anodic currents obtained from the sediment could be related to some of the following processes: (a) the formation of an aeration cell resulting from the low diffusion of oxygen beyond the water/sediment interface (11), (b) the generation of a concentration cell based on the accumulation of reduced compounds in the anoxic sediment, and (c) the enrichment in microorganisms able to exchange electrons with the graphite electrode (25, 26).

In nonstabilized sediment, oxygen exhaustion is expected to occur, while reduced compounds started to accumulate in the sediment driving the anodes potential to negative values (Figure 1b). Nevertheless, these potential-determining processes were not able to polarize SS to the selected protection potential as far as 50 days from anode installation (Figure 1b). This lag period to produce the required current showed the minor contribution of the aeration cell and the need for the accumulation of reduced compounds in the sediments to have operative anodes.

Sulfide minerals constitute one of the most abundant reductants in marine sediments (27) and have been related to the potential adopted by buried graphite electrodes in anoxic sediments (27). Indeed, the oxidation of reduced sulfur compounds has been proposed as the main energy-providing process in sediment fuel cells (27, 28). Both changes in the anode potential (Figure 1b) and voltammetries on nonconnected graphite electrodes (Figure 3a) point to the accumulation of a reduced compound in the sediment. This compound would cathodically polarize the anodes and can be electrochemically oxidized with the application of overpotentials. Tender et al. (28) discussed the role of sulfide oxidation in energy generation, and more recently, Ryckelynck et al. (27) proposed that the oxidation of sulfide minerals is the main current source in the sediments. Cyclic voltammetry reveals that, when oxidized products from the process in Figure 3 are electrochemically reduced and reoxidized again (Figure 4), the wave forms closely resemble those obtained on pyrite electrodes (29), suggesting that sulfide minerals are involved in the electrode processes detected here. In this way, reduction waves at potentials lower than -0.6 V have been assigned by Mycroft et al. (29) to pyrite reduction, whereas oxidation peaks found between -0.4 and 0.1 V have been related to the occurrence of various processes that include sulfide and polysulfide oxidation to sulfur (29, 30). Additionally, a redox potential of -0.447 V (SCE) can be calculated for the oxidation of sulfide to elemental sulfur (at pH 7.1, 20 °C, sulfide concentration $= 4 \times 10^{-3}$ M (28), and a standard potential versus the normal hydrogen electrode, $E_{0,NHE} = -0.139$ V (31)) using the Nernst equation. This value is in close agreement with the half-cell potential for the processes in Figure 4, which also suggest the participation of reduced sulfur in those processes. The oxidation waves of sulfide and polysulfide compounds overlap at potentials ranging from -0.4 to 0.1 V (Figure 4). Since anodes were polarized to a potential of around -0.35 V during the protection experiments (Figure 1), these oxidations are the most probable candidates for the provision of current. Ryckelinck et al. (2005) (27) also discussed the role of sulfur oxidation to sulfate as an electron-providing reaction. Nevertheless, sulfur oxidation to the oxianions requires polarization to potentials beyond 0.45 V (29, 30). Cathodic protection was implemented in this work in a manner such that the graphite electrodes were never polarized to potentials higher than -0.30 ± 0.02 V (Figure 2). As a consequence, protection currents are thought to be mainly provided by the oxidation of S^{2-} compounds to polysulfides, elemental sulfur, or both, in this case. The EDX analysis of graphite electrodes showed the presence of localized mineral deposits with S/Fe ratios as high as 2 on

electrodes that were connected to SS cathodes (see the Supporting Information). In addition, the absence of oxidation peaks during the first forward scan of voltammetries on these electrodes (inset Figure 4b) indicates that reduced sulfur compounds at the interface are not longer present, showing that most of them were oxidized to elemental sulfur during cathodic protection.

The presence of sulfur deposits has been described to occur on the anodes of sediment fuel cells that were operated with a small loading resistance, in which anodes were polarized to near 0.0 V (27, 28). Sulfur has been related to the enrichment in bacteria that can obtain energy for growth from the disproportionation of S^0 (32). A possible role of the electrode as the electron acceptor has been postulated in that case (32). Voltammetric reduction peaks on active anodes (Figure 4b) are thought to be caused by the reduction of sulfur compounds deposited on graphite electrodes as a consequence of current demand during cathodic protection. Nevertheless, the amount of charge transferred during reduction was far from that registered on nonconnected electrodes (Figure 4a). This could be probably related to the microbiologically catalyzed oxidation of sulfur to sulfate (27).

During recent years, the participation of electrochemically active microorganisms in the generation of electric current has been proposed and increasingly studied (25, 28, 33, 34). Bond et al. (25) reported an enrichment in bacteria belonging to the family Geobacteraceae on energy-harvesting anodes. They showed that these microorganisms can conserve energy using the electrode as an electron acceptor. Tender et al. (28) calculated that sulfide oxidation is not enough to cover the current output that they obtained from fuel cells and proposed that electrochemically active microorganisms may be participating in energy generation. From results presented here, it is not possible to determine if electrode-reducing microorganisms are involved in the generation of protection currents. Nevertheless, the absence of sulfur compound oxidation peaks in the voltammetry of active anodes (Figure 3b) indicates that, because of the transport limitation on sulfide mineral oxidation, a net electron demand at the anode's surface may exist providing a positive selection force for electrode-reducing microorganisms in the sediment. In addition, surface polarization has been shown to induce the growth of bacteria on a conducting surface in an attached state (35). Microbial electrochemical activity in fuel cell devices has been found to be sometimes evidenced by poorly defined oxidation peaks that reach a plateau with increasing potential (34, 36). Results in Figure 3b include a plateau with complex undefined oxidation waves, together with an overall current increase with time, that could be a consequence of the development of an electrochemically active microbial population on the anode.

From the results presented here, the polarization of SS at potentials in the passivity region (i.e., -0.2 V) by coupling with buried graphite anodes is proposed as a new approach to the classical cathodic protection method. It could be implemented in seawater applications as those found in the offshore oil production industry or in the construction of submarine emissaries for municipal wastewater disposal, among others. Once installed, it should need minimal requirements for maintenance with a very low cost. Finally and most importantly, it would have significant environmental benefits since it is based on an immense and renewable energy source and does not produce aggressive emissions to the environment.

Supporting Information Available

A schematic representation of the experimental setup (Figure S1), a cathodic polarization analysis of stainless steel cathodes (Figure S2), and the results of SEM and EDX analysis on the anodes surface (Figures S3 and S4, respectively). This material is available free of charge via the Internet at http://pubs.acs.org.

Literature Cited

(1) Mollica, A.; Trevis, A.; Traverso, E.; Ventura, G.; Decarolis, G.; Dellepiane, R. Cathodic performance of stainless-steels in natural seawater as a function of microorganism settlement and temperature. *Corrosion* **1989**, *45* (1), 48−56.

(2) Salvago, G.; Magagnin, L. Biofilm effect on the cathodic and anodic processes on stainless steel in seawater near the corrosion potential: Part 1−Corrosion potential. *Corrosion* **2001**, *57* (8), 680−692.

(3) Scotto, V.; Lai, M. E. The ennoblement of stainless steels in seawater: A likely explanation coming from the field. *Corros. Sci.* **1998**, *40* (6), 1007−1018.

(4) L'Hostis, V.; Dagbert, C.; Feron, D.; Galland, J. Models for the electrochemical behaviour of stainless steels in natural seawater. Presented at the 15th International Corrosion Congress, Grenade, Spain, 2002.

(5) Dickinson, W. H.; Caccavo, J. F.; Lewandowski, Z. The ennoblement of stainless steel by manganic oxide biofouling. *Corros. Sci.* **1996**, *38* (8), 1407−1422.

(6) Dexter, S. C. Biofouling and biocorrosion. *Bull. Electrochem.* **1996**, *12* (1−2), 1−7.

(7) Busalmen, J. P.; Vazquez, M.; de Sanchez, S. R. New evidences on the catalase mechanism of microbial corrosion. *Electrochim. Acta* **2002**, *47* (12), 1857−1865.

(8) Heidersbach, R. H. Cathodic protection. In *Corrosion*, 9th ed.; Davis, J. R., Ed.; ASM International: Ohio, 1987; Vol. 13, pp 467−477.

(9) Reimers, C. E.; Tender, L. M.; Fertig, S.; Wang, W. Harvesting energy from the marine sediment−water interface. *Environ. Sci. Technol.* **2001**, *35* (1), 192−195.

(10) Scotto, V.; Dicintio, R.; Marcenaro, G. The influence of marine aerobic microbial film on stainless-steel corrosion behavior. *Corros. Sci.* **1985**, *25* (3), 185−194.

(11) Jones, D. *Principles and Prevention of Corrosion*; MacMillan: New York, 1992.

(12) Salvago, G.; Bollini, G. Localized corrosion probability in stainless steels after cathodic protection in seawater. *Corrosion* **1999**, *55* (4), 397−405.

(13) Baptista, W.; Pimenta, G. Cathodic protection against crevice corrosion of high-alloy steel in seawater. *Mater. Perform.* **1995**, *34* (10), 29−32.

(14) deSaravia, S. G. G.; deMele, M. F. L.; Videla, H. A.; Edyvean, R. G. J. Bacterial biofilms on cathodically protected stainless steel. *Biofouling* **1997**, *11* (1), 1−17.

(15) Guezennec, J. G. Cathodic protection and microbially induced corrosion. *Int. Biodeterior. Biodegrad.* **1994**, *34* (3−4), 275−288.

(16) Dexter, S. C.; Lin, S.-H. Effect of marine biofilms on cathodic protection. *Int. Biodeterior. Biodegrad.* **1992**, *29* (3−4), 231−249.

(17) Dexter, S. C.; LaFontaine, J. P. Effect of natural marine biofilms on galvanic corrosion. *Corrosion* **1998**, *54* (11), 851−861.

(18) Johnsen, R.; Bardal, E. Cathodic properties of different stainless-steels in natural seawater. *Corrosion* **1985**, *41* (5), 296−302.

(19) Hinds, G.; Zhao, J.; Griffiths, A. J.; Turnbull, A. Hydrogen diffusion in super 13% chromium martensitic stainless steel. *Corrosion* **2005**, *61* (4), 348−354.

(20) Eliassen, S. New concept for cathodic protection of offshore pipelines to reduce hydrogen induced stress cracking (HISC) in high strength 13% Cr stainless steels. *Corros. Eng. Sci. Technol.* **2004**, *39* (1), 31−37.

(21) Babic, R.; Metikoshukovic, M. Oxygen reduction on stainless-steel. *J. Appl. Electrochem.* **1993**, *23* (4), 352−357.

(22) Little, B.; Wagner, P.; Duquette, D. Microbiologically induced increase in corrosion current-density of stainless-steel under cathodic protection. *Corrosion* **1988**, *44* (5), 270−274.

(23) Bergel, A.; Feron, D.; Mollica, A. Catalysis of oxygen reduction in PEM fuel cell by seawater biofilm. *Electrochem. Commun.* **2005**, *7* (9), 900−904.

(24) Lowy, D. A.; Tender, L. M.; Zeikus, J. G.; Park, D. H.; Lovley, D. R. Harvesting energy from the marine sediment−water interface II: Kinetic activity of anode materials. *Biosens. Bioelectron.* **2006**, *21* (11), 2058.

(25) Bond, D. R.; Holmes, D. E.; Tender, L. M.; Lovley, D. R. Electrode-reducing microorganisms that harvest energy from marine sediments. *Science* **2002**, *295* (5554), 483−485.

(26) Holmes, D. E.; Bond, D. R.; Lovley, D. R. Electron transfer by *Desulfobulbus propionicus* to Fe(III) and graphite electrodes. *Appl. Environ. Microbiol.* **2004**, *70* (2), 1234−1237.

(27) Ryckelynck, N.; Stecher, H. A.; Reimers, C. E. Understanding the anodic mechanism of a seafloor fuel cell: Interactions between geochemistry and microbial activity. *Biogeochemistry* **2005**, *76* (1), 113−139.

(28) Tender, L. M.; Reimers, C. E.; Stecher, H. A., III; Holmes, D. E.; Bond, D. R.; Lowy, D. A.; Pilobello, K.; Fertig, S. J.; Lovley, D. R. Harnessing microbially generated power on the seafloor. *Nat. Biotechnol.* **2002**, *20* (8), 821−825.

(29) Mycroft, J. R.; Bancroft, G. M.; McIntyre, N. S.; Lorimer, J. W.; Hill, I. R. Detection of sulphur and polysulphides on electrochemically oxidized pyrite surfaces by X-ray photoelectron spectroscopy and Raman spectroscopy. *J. Electroanal. Chem.* **1990**, *292* (1−2), 139.

(30) Hamilton, I. C.; Woods, R. An investigation of surface oxidation of pyrite and pyrrhotite by linear potential sweep voltammetry. *J. Electroanal. Chem.* **1981**, *118*, 327.

(31) Stumm, W.; Morgan, J. J. *Aquatic Chemistry: An Introduction Emphasizing Chemical Equilibria in Natural Waters;* Wiley & Sons: New York, 1981.

(32) Holmes, D. E.; Bond, D. R.; O'Neill, R. A.; Reimers, C. E.; Tender, L. R.; Lovley, D. R. Microbial communities associated with electrodes harvesting electricity from a variety of aquatic sediments. *Microb. Ecol.* **2004**, *48* (2), 178−190.

(33) Bond, D. R.; Lovley, D. R. Electricity production by *Geobacter sulfurreducens* attached to electrodes. *Appl. Environ. Microbiol.* **2003**, *69* (3), 1548−55.

(34) Kim, H. J.; Park, H. S.; Hyun, M. S.; Chang, I. S.; Kim, M.; Kim, B. H. A mediator-less microbial fuel cell using a metal reducing bacterium, *Shewanella putrefaciens. Enzyme Microb. Technol.* **2002**, *30* (2), 145−152.

(35) Busalmen, J. P.; de Sanchez, S. R. Electrochemical polarization-induced changes in the growth of individual cells and biofilms of *Pseudomonas fluorescens* (ATCC 17552). *Appl. Environ. Microbiol.* **2005**, *71* (10), 6235−6240.

(36) Rabaey, K.; Boon, N.; Siciliano, S. D.; Verhaege, M.; Verstraete, W. Biofuel cells select for microbial consortia that self-mediate electron transfer. *Appl. Environ. Microbiol.* **2004**, *70* (9), 5373−5382.